

Subsystem Thermalization Hypothesis in Quantum Spin Chains with Conserved Charges

Feng-Li Lin,^{1,*} Jhh-Jing Hong,^{1,†} and Ching-Yu Huang^{2,‡}

¹*Department of Physics,
National Taiwan Normal University, Taipei, 11677, Taiwan*

²*Department of Applied Physics,
Tunghai University, Taichung 40704, Taiwan*

(Dated: December 16, 2024)

We consider the thermalization hypothesis of pure states in quantum Ising chain with Z_2 symmetry, XXZ chain with $U(1)$ symmetry, and XXX chain with $SU(2)$ symmetries. Two kinds of pure states are considered: the energy eigenstates and the typical states evolved unitarily from the random product states for a long enough period. We further group the typical states by their expectation values of the conserved charges and consider the fine-grained thermalization hypothesis. We compare the locally (subsystem) reduced states of typical states/eigenstates with the ones of the corresponding thermal ensemble states. Besides the usual thermal ensembles such as the (micro-)canonical ensemble without conserved charges and the generalized Gibbs ensemble (GGE) with all conserved charges included, we also consider the so-called partial-GGEs (p-GGEs), which include only part of the conserved charges in the thermal ensemble. Moreover, in the framework of p-GGE, the Hamiltonian and other conserved charges are on an equal footing. The introduction of p-GGEs extends quantum thermalization to a more general scope. The validity of the subsystem thermalization hypothesis can be quantified by the smallness of the relative entropy of the reduced states obtained from the GGE/p-GGE and the typical states/eigenstates. We examine the validity of the thermalization hypothesis by numerically studying the relative entropy demographics. We show that the thermalization hypothesis holds generically for the small enough subsystems for various p-GGEs. Thus, our framework extends the universality of quantum thermalization.

CONTENTS

I. Introduction	1
II. Thermalization of Quantum Systems with Conserved Charges	2
III. Thermalization demographics for quantum Ising spin chains	6
A. Demographics of typical-state thermalization	6
B. Demographics of almost superselection-state thermalization	7
C. Demographics of eigenstate thermalization	9
IV. Thermalization demographics of quantum spin-1/2 XXZ chains with $U(1)$ symmetry	9
V. Thermalization demographics of quantum spin-1/2 XXZ chains with $SU(2)$ symmetry	11
A. Demographics of typical-state thermalization	11
B. Demographics of eigenstate thermalization	13
VI. Conclusion	13
Acknowledgments	13
A. Typical-state thermalization demographics of the XXZ chain with $U(1)$ conserved charges	13
References	14

I. INTRODUCTION

The thermalization of a classical many-body system is dictated by the second law of thermodynamics and is also deeply related to chaos and ergodicity. For quantum systems, a long-evolved open subsystem interacting with the environment displays similar thermalization behaviors, which can also be understood as the spreading of entanglement across the boundary between the subsystem and the environment. On the other hand, the isolated quantum system evolves unitarily, and it seems unable to thermalize. Among them, the energy eigenstate is stationary and should not be able to thermalize. Inspired by von Neuman's idea of trying to generalize the ergodicity theorem to quantum mechanics [1], the so-called eigenstate thermalization hypothesis (ETH) was proposed [2–4], which states that the expectation value of any local observable with respect to an energy eigenstate of medium energy is approximately by the microcanonical ensemble average. Since then, thermalization of isolated quantum systems has been intensively studied in the past decades; see [5–9] and the references therein. Surprisingly, ETH seems quite general. The ETH implies that the reduced state in a small region of an energy eigenstate can be approximated by the (reduced) state of some thermal ensemble state, such as the (micro-)canonical ensemble. This can be seen as the subsystem version of ETH [10–12], i.e., by treating a local region as a subsystem of the whole system. The validity of (subsystem) ETH implies that an energy eigenstate locally looks like thermal.

Energy eigenstates comprise only a tiny portion of the total Hilbert space of an isolated many-body system. It is natural to ask if the (subsystem) thermalization also happens to the typical states, which can be practically obtained by the long-time evolution of some initial non-eigenstate. This was proposed in [13] as the *canonical typicality* to conjecture that a typi-

* fengli.lin@gmail.com

† hongjhhjing06132061@gmail.com

‡ cyhuangphy@thu.edu.tw

cal state is locally thermal. The subsystem thermalization of a typical state of an isolated system may be understood by treating the subsystem as an open system surrounded by the rest. The open system will be expected to equilibrate with the surrounding environment due to their mutual interaction to grow and spread the entanglement across the boundary. Despite that, the equilibrium state may not be some thermal ensemble state, but some pointer state preferred by the environment's einselection [14]. This is expected because the environment here is just complementary to the subsystem of a typical state and may not behave as a thermal bath. However, inspired by the subsystem ETH, the reduced state to the subsystem of a typical state can look like the reduced state of some thermal ensemble state [15, 16].

It has been known that the above (subsystem) ETH fails¹ for the integrable systems [12, 17–22] due to the infinite number of conserved charges prohibiting quantum chaos for thermalization. One expects the ETH will hold when compared with the reduced state of the generalized Gibbs ensemble (GGE), including all the conserved charges [23, 24]. However, such GGE is hard to implement due to the infinite number of conserved charges. Similarly, we may expect that the integrable systems' typical states may not be thermalized if not compared with GGE. This then raises the issue of the role of the conserved charges in the thermalization of energy eigenstates or typical states.

With the additional conserved charges other than Hamiltonian, there are more options when considering the thermalization hypothesis in various aspects. Firstly, the energy eigenstates will be classified into the superselection sectors of the conserved charges. When considering ETH, we can choose to restrict to the superselection sectors or not. We can also generalize the concept of superselection sectors to the typical states. Although the typical states, in general, are not the eigenstates of energy and charges, we can still classify them into almost superselection by their expectation values of the charges.

Secondly, we can choose different thermal ensemble states to examine the thermalization hypothesis for either eigenstates or typical states. A conserved quantity and its chemical potential come as a conjugate pair when constructing a thermal ensemble, i.e., we can fix either charge or chemical potential, but not both. Or, we can ignore both. For example, when there is no conserved quantity other than the Hamiltonian, we can either fix energy to yield a microcanonical ensemble state or fix (inverse) temperature to yield a canonical ensemble state. We can adopt either to consider the thermalization hypothesis. Thus, with more conserved quantities, we can fix either one for each conjugate pair or ignore both to yield different thermal ensembles. If we fix all the chemical potential, including the inverse temperature, we will obtain the GGE. Otherwise, we will obtain the so-called partial-GGE (p-GGE). Finally, as we have the option of choosing (almost) superselection sectors for the quantum states and the p-GGEs, we should not just ex-

amine the thermalization of a single state but shall evaluate the thermalization hypothesis by the Demographics of the relative entropy measures for a given set of states in some (almost) superselection sector and a chosen p-GGE.

In this paper, we will study this issue by considering the nonintegrable spin chain systems with either discrete or continuous Abelian and non-Abelian symmetries. In particular, the thermalization hypothesis for the system with non-Abelian conserved charges has been studied recently [25–30], among which a GGE-like state called non-Abelian thermal state (NATS) has been proposed for ETH. In our framework with p-GGE states, we will numerically study the subsystem thermalization hypothesis of the typical states, (almost-)superselection states, and energy eigenstates of the quantum Ising and XXZ chains by comparing their locally reduced states with the ones of various p-GGE thermal states. The demographics of such comparisons will tell us how general the thermalization of isolated quantum systems with conserved charges can be.

The rest of the paper is organized as follows. In section II, we will sketch our framework for examining the subsystem thermalization hypothesis and its relation with the generalized second law of thermodynamics and our numerical implementation methodology. We then present our numerical results of the thermalization demographics for the Ising chain with Z_2 conserved charges, the XXZ chain with $U(1)$ charges, and the XXX chain with $SU(2)$ charges, in section III, IV and V, respectively. We will see that the subsystem thermalization hypothesis holds well for the local region of small sizes in most cases. Finally, we conclude our paper in section VI. To make the main text more concise, we put some typical-state thermalization demographics for the cases of XXZ chain in Appendix A.

II. THERMALIZATION OF QUANTUM SYSTEMS WITH CONSERVED CHARGES

We want to consider the thermalization of typical states in a system with conserved charges. In this section, we first review the basics of thermalization for systems without conserved charges and then generalize to those with conserved charges.

There are many ways to consider the thermalization of a quantum system, and the key point is to pick up a thermal ensemble state to compare with the given typical state on the agreement of local observables or, more directly, the reduced density matrices of some local regions. Take the eigenstate thermalization hypothesis (ETH) [2, 4] as an example. One compares a given energy eigenstate $|E\rangle$ of energy E with some thermal ensemble state, which can either be a micro-canonical or canonical ensemble. It is natural to choose the energy of the micro-canonical ensemble to center around E with a small window $\Delta E \leq E$. The ETH works if the local observables' expectation values agree well with the micro-canonical ensemble's thermal averages. That is

$$\langle E|\mathcal{O}|E\rangle \simeq \langle \mathcal{O} \rangle_{\text{mce}} \quad (1)$$

for a complete set of local observables $\{\mathcal{O}\}$, where mce de-

¹ Or, it holds only weakly (weak ETH) [12, 17–19], i.e., the distance between two reduced states vanishes by the power law of the number of degrees of freedom, not by the exponential decay as for the strong ETH.

notes the abbreviation of micro-canonical ensemble. On the other hand, the canonical ensemble

$$\rho_{\text{ce}} = \frac{e^{-\beta H}}{\text{Tr} e^{-\beta H}} \quad (2)$$

is specified by the system's Hamiltonian H and the inverse temperature β . The latter should be fixed by requiring the average energy to be E , i.e.,

$$E = \langle E|H|E \rangle = \text{Tr}[\rho_{\text{ce}}H]. \quad (3)$$

The ETH holds if the reduced density matrices for a small local region A (with its complement denoted by \bar{A}) agree, i.e.,

$$S[\text{Tr}_{\bar{A}}|E\rangle\langle E| \parallel \text{Tr}_{\bar{A}}\rho_{\text{ce}}] \simeq 0 \quad (4)$$

where $S[\rho_1 \parallel \rho_2]$ is the relative entropy between ρ_1 and ρ_2 . This is the so-called subsystem ETH [10–12]. A tighter measure than the relative entropy for the difference between ρ_1 and ρ_2 is the trace distance $t_{12} := \text{tr}|\rho_1 - \rho_2|$. However, it is more difficult to evaluate. Despite that, by Pinsker's inequality

$$t_{12}^2 \leq 2S[\rho_1 \parallel \rho_2], \quad (5)$$

we can evaluate the relative entropy as the upper bound to the trace distance.

Besides ETH, one can consider the thermalization for a typical pure state $|\Psi\rangle$, which is not an eigenstate or a product state. Then, the canonical ensemble or its β can be fixed by

$$\langle \Psi|H|\Psi \rangle = \text{Tr}[\rho_{\text{ce}}H] \quad (6)$$

and the typical state $|\Psi\rangle$ behaves thermally inside A if

$$S[\text{Tr}_{\bar{A}}|\Psi\rangle\langle\Psi| \parallel \text{Tr}_{\bar{A}}\rho_{\text{ce}}] \simeq 0. \quad (7)$$

In [31], the above thermalization hypothesis is proposed and termed generic ETH, which has been checked for the long-time evolved product states. In this work, we call it the subsystem thermalization hypothesis, a generalization of subsystem ETH to include both eigenstates and typical states. For the subsystem thermalization hypothesis to hold, the size of A should be far smaller than the system's. As A increases its size to some critical one denoted by A_c , one should expect the failure of the subsystem thermalization hypothesis. Thus, A_c can be used to characterize the robustness of the thermalization hypothesis and should be system-dependent. For example, one will wonder how the symmetries of the system affect A_c .

We can generalize the above subsystem thermalization hypothesis to systems with conserved charges $\{Q_I\}$ where I labels the charges. For simplicity, we set $Q_0 = H$ so that $[Q_0, Q_{I \neq 0}] = 0$. In statistical mechanics, the conserved charge Q_I and its corresponding chemical potential β_I form the conjugate pair. When fixing a thermal ensemble, we can fix either Q_I or β_I . Denote the set of fixed charges as $\{Q_a\}$ and the set of fixed chemical potentials as $\{\beta_j\}$. These two

sets are mutually exclusive, i.e., $\{a\} \cap \{j\} = \emptyset$. However, there are remaining charges labeled by index γ , for which we fix neither Q_γ nor β_γ . Note that $\{a\} \cup \{j\} \cup \{\gamma\} = \{I\}$. With the above classification of the conserved charges, we define the so-called partial generalized Gibbs ensemble (p-GGE) thermal state as

$$\rho_{\{j\}} = \frac{e^{-\sum_j \beta_j Q_j}}{\text{Tr} e^{-\sum_j \beta_j Q_j}} \quad \forall j. \quad (8)$$

If $\{j\} = \{I\}$, it is just the GGE state, i.e., $\rho_{\text{gge}} = \rho_{\{I\}}$.

After introducing the p-GGE, the subsystem thermalization hypothesis can be extended to the systems with conserved charges. For a given state $|\Psi\rangle$, a chosen p-GGE ensemble state can be fixed by requiring

$$\langle \Psi|Q_j|\Psi \rangle = \text{Tr}[\rho_{\{j\}}Q_j] \quad \forall j \quad (9)$$

to solve for $\{\beta_j\}$ to fix $\rho_{\{j\}}$. The subsystem thermalization hypothesis for the chosen p-GGE holds if

$$S_A := S[\text{Tr}_{\bar{A}}|\Psi\rangle\langle\Psi| \parallel \text{Tr}_{\bar{A}}\rho_{\{j\}}] \simeq 0. \quad (10)$$

This scheme of subsystem thermalization hypothesis for the systems with conserved charges is summarized in Fig. 1.

As the construction of p-GGE only involves the set of conserved charges labeled by $\{j\}$, this leads to the following variations of the subsystem thermalization hypothesis by picking up different sets of states $\{|\Psi\rangle\}$ related or unrelated to the remaining sets of conserved charges labeled by $\{a\}$ or $\{\gamma\}$.

1. Typical-state thermalization. In this case, the states $\{|\Psi\rangle\}$ do not belong to any superselection sector associated with $\{Q_I\}$.
2. Extended ETH. In this case, we choose $\{Q_a\}$ to be mutually commuting and examine the thermalization hypothesis of their eigenstates $\{|q_a\rangle\}$, defined by

$$Q_a|q_b\rangle = q_a|q_b\rangle \quad \forall a. \quad (11)$$

3. Thermalization of the almost $\{Q_a\}$ -superselection states $\{|\Psi^{\{a\}}\rangle\}$, defined by

$$\langle \Psi^{\{a\}}|Q_a|\Psi^{\{a\}} \rangle \simeq \langle Q_a \rangle \quad \forall a \quad (12)$$

for a given set $\{\langle Q_a \rangle\}$. This case is the fine-grained version of the typical-state thermalization hypothesis by subdividing the typical states into almost superselection sectors specified by $\langle Q_a \rangle$.

Note that we call $\{|\Psi^{\{a\}}\rangle\}$ the almost superselection states to distinguish from the genuine superselection states, i.e., the eigenstates of $\{Q_a\}$. The latter cannot be defined if $\{Q_a\}$ are not mutually commuting.

Besides the above choices of states to test the thermalization hypothesis, we have some remarks to extend the scope of the subsystem thermalization hypothesis further, which we will consider in this paper.

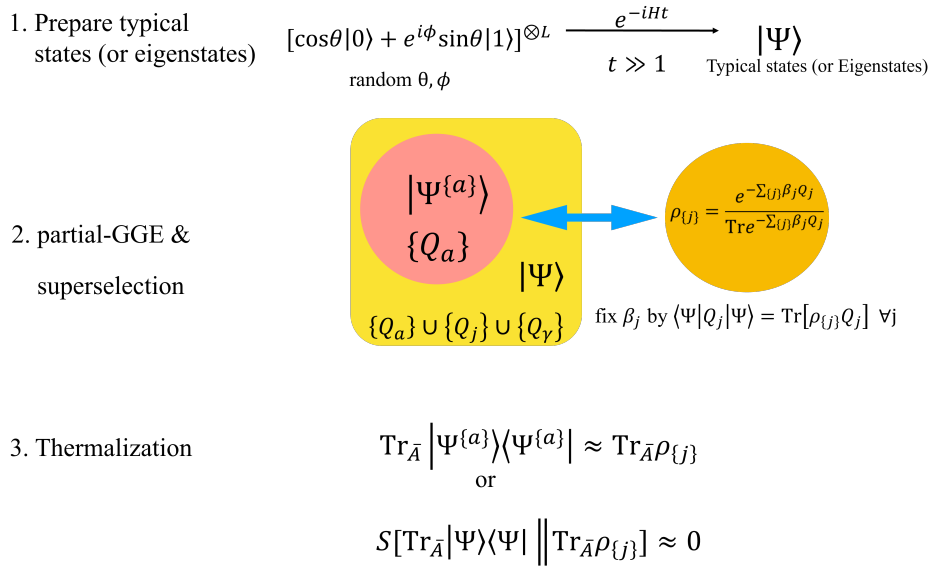


FIG. 1. Scheme of subsystem thermalization hypothesis for the systems with conserved charges by comparing the reduced states on a region A of a typical state (or eigenstate) and a partial-GGE state.

- Even though the Hamiltonian Q_0 is a special one among the conserved charges, it is interesting to consider the p-GGE with Q_0 excluded in the set $\{j\}$.
- As the p-GGE is constructed by fixing $\{\beta_j\}$ instead of $\{Q_j\}$, we can consider the p-GGE for either commuting or non-commuting $\{Q_j\}$. The latter can be applied to systems with non-Abelian symmetry, such as the XXX chains, and can be compared with the GGE one, which is the NATS proposed and studied in [26–29].
- When considering the subsystem thermalization hypothesis for the non-Abelian symmetry systems, we can also choose the almost superselection states $\{|\Psi^{a}\rangle\}$ for the non-commuting $\{Q_a\}$, or the eigenstates $\{|q_a\rangle\}$ for commuting $\{Q_a\}$. These provide new ways to examine the thermalization hypothesis of typical states and ETH with non-Abelian symmetries.
- The framework discussed so far should be applied to systems with continuous or discrete symmetries. The eigenvalues of charges of discrete symmetries take only discrete values. However, the values of $\{Q_a\}$ of (12) for the almost superselection states can also take continuous values for discrete symmetries.
- When considering the integrable models, it is impractical to include all the conserved charges in the hypothetical thermal ensemble states. In this case, we can form a p-GGE of a small set $\{a\}$ to test the thermalization hypothesis and ignore most integrable charges, i.e., a large set of γ .
- With the numerical implementation to check the thermalization hypothesis by (10), we can study the dependence of $S[\text{Tr}_{\bar{A}} |\Psi\rangle\langle\Psi| \parallel \text{Tr}_{\bar{A}} \rho_{\{j\}}]$ on the size of A .

The main goal of this paper is to study the thermalization demographic for each possible scenario discussed above and see if the thermalization is generic enough. The relative entropy is adopted to characterize the thermalization demographics, and its notations used later for various scenarios are summarized in Table I.

In summary, we will consider the subsystem thermalization hypothesis for two types of spin-1/2 chains with conserved charges: the quantum Ising chains and the quantum XXZ chains. The nonintegrable Ising chains have a conserved Z_2 charge. Interestingly, as we will see, the subsystem thermalization hypothesis also works for the p-GGE of discrete charge. The symmetries of XXZ chains are richer than the Ising's, but we will mainly focus on $U(1)$ and $SU(2)$. The latter is non-Abelian, and it is interesting to examine the subsystem thermalization hypothesis for typical states or eigenstates of systems with such non-Abelian symmetries by comparing them with p-GGE.

That is, we construct an extensive set of eigenstates or typical states $\{\Phi\}$ labeled by $\{Q_a\}$, and choose some chosen p-GGE labeled by $\{\beta_j\}$. We then present the demographic distribution of the relative entropy of $S[\text{Tr}_{\bar{A}} |\Psi\rangle\langle\Psi| \parallel \text{Tr}_{\bar{A}} \rho_{\{j\}}]$ as functions of $\{Q_a\}$ and $\{\beta_j\}$. By examining these thermalization demographics, we can examine the validity of the subsystem thermalization hypothesis.

Before presenting the thermalization demographics, we have two remarks about the generality of quantum thermalization and how to prepare the typical states numerically. Firstly, we consider the generality of quantum thermalization by extending an argument for GGE in [32] to the cases for p-GGE. This can provide some understanding of quantum thermalization by the second-law-like argument. The key idea of [32] is to define the so-called free entropy for a generic state ρ for a

	GGE	p-GGE	p-GGE (almost)
typical state	S_A^t	S_A^t	S_A^a
eigenstate	S_A^e	S_A^e	

TABLE I. Notations of realtive entropy S_A defined in (10) and used in different scenarios of the thermalization hypothesis. The superscript t denotes the typical state, e is the eigenstate, and a is the almost superselection or just superselection state. The size of A ranges from one site to half of the spin chain.

given set of chemical potentials $\{\beta_j\}$ as follows [32],

$$\tilde{F}[\rho] = \sum_j \beta_j \text{Tr}(\rho Q_j) - S[\rho] \quad (13)$$

where $S[\rho] := -\text{Tr}[\rho \ln \rho]$ is the von Neumann entropy of ρ . Note that

$$\tilde{F}[\rho_{\{j\}}] = -\ln \text{Tr} e^{-\sum_j \beta_j Q_j}. \quad (14)$$

It can be shown that [32]

$$\tilde{F}[\rho] - \tilde{F}[\rho_{\{j\}}] = S[\rho || \rho_{\{j\}}]. \quad (15)$$

Thus, p-GGE is the state of minimal free entropy because $S[\rho || \rho_{\{j\}}] \geq 0$, which can be shown to be equivalent to maximizing von Neumann entropy with fixed $\text{Tr}(\rho Q_j)$ for all j [32]. By (15), the thermalization condition (10) can also be understood as the free entropy difference for the reduced states of the region A inherited from $|\Psi\rangle\langle\Psi|$ and ρ_{gge} , respectively.

One can put the above discussion in the context of the resource theory of quantum thermodynamics [33]. A resource theory is determined by two key ingredients: the free states and the free operations. Given that, one also needs a monotone quantity to define the condition for state transitions. To be specific in quantum thermodynamics, the p-GGE states described above are the free states, and the free entropy defined above is the monotone so that the state transition: $\rho \rightarrow \rho'$ is possible only if

$$\Delta\tilde{F} := \tilde{F}[\rho'] - \tilde{F}[\rho] \leq 0. \quad (16)$$

This is the statement of the second law of thermodynamics. Given free entropy as the monotone for state transitions, the free operations are just the evolution conserving Q_j 's, e.g., $U(t) = e^{-it \sum_j \alpha_j Q_j}$, which will not change the free entropy. Otherwise, the operations are the so-called thermal operations (TOs) [33].

Secondly, we will mention how we numerically prepare and define the typical states. The subsystem thermalization hypothesis can work for the systems even without taking the thermodynamic limit as long as the subsystem size is far smaller than the system's. We will mainly adopt the exact diagonalization method (ED) to find the eigenstates of the spin chain models with the size of about ten sites. We will also use it to evolve the initial product states to prepare

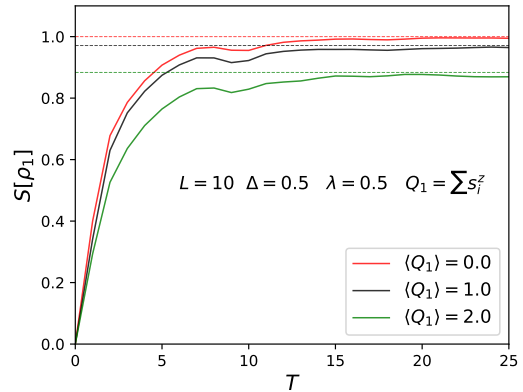


FIG. 2. The evolving pattern of one-site entanglement entropy $S[\rho_1]$ of a 10-site nonintegrable XXZ chain specified by (21) and (22). This model has a $U(1)$ conserved charge denoted by Q_1 , see (23). Each solid line represents the average of $S[\rho_1]$ over 500 states at each time step, which are evolved from the initial product states with fixed $\langle Q_1 \rangle$. In this figure, we consider $\langle Q_1 \rangle = 0.0$ (red), 1.0 (blue) and 2.0 (green). The dashed lines are the values of $S[\rho_1]$ of the corresponding GGE states. The result shows that values of $S[\rho_1]$ saturate to a non-thermal value around $T = 25$.

the typical states for checking the subsystem thermalization hypothesis. Explicitly, we first prepare the initial entangled state by $|\psi\rangle = \otimes_{i=1}^L \left(\cos(\theta_i/2)|0\rangle + e^{i\phi_i} \sin(\theta_i/2)|1\rangle \right)$ with $\theta_i \in [0, \pi]$, $\phi_i \in [0, 2\pi]$ generated uniformly and randomly. Then, we evolve these states with the Hamiltonian of the spin chain model by ED for chains of 10 sites or so. Although 10-site chains seem small, as we will see, it is enough to achieve the subsystem thermalization at least for $A = 1$. One will expect A_c to increase as the system size increases. This can be a future study by using matrix product states (MPS) to obtain the typical states for the longer chains. In our previous work [34], we have shown it is possible to accurately evolve product states or prepare thermal states using matrix product states (MPS) for spin chains of a few hundred sites.

There is no unique definition of a typical state. In this work, we adopt the following definition used in [31]: its entanglement entropy of a single site with the rest of the spin chain, denoted by $S[\rho_1]$, is about the maximal value given by the time evolution of an initial product state. This will exclude some transient states, which may not be typical regarding entanglement spreading. We give an example for this construction by considering a ten-site nonintegrable XXZ spin chain with a $U(1)$ conserved charge Q_1 . We then use ED to evolve a randomly generated product state with zero $S[\rho_1]$ but fixed $\langle Q_1 \rangle$. In Fig. 2, we show the evolving pattern of the averaged $S[\rho_1]$ over 500 initial states. The result shows that the (averaged) $S[\rho_1]$ values saturate to a maximal after $T \simeq 25$. However, these maximal values may differ from those given by the corresponding GGE states. In this work, the typical states we collect for the demographic of subsystem thermalization hypothesis are obtained by evolving the randomly generated product states with time duration $T = 1000$. This should be

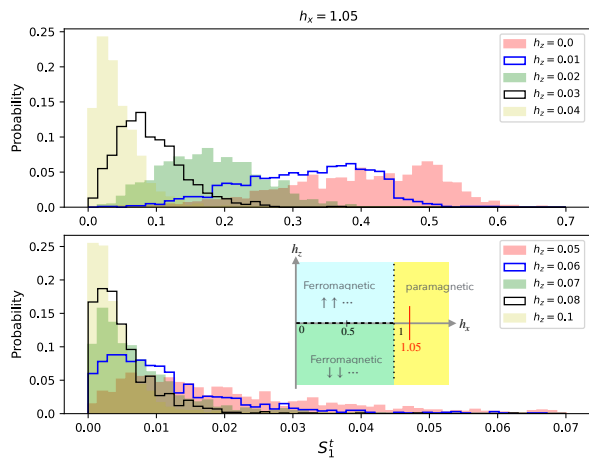


FIG. 3. Patterns of typical-state thermalization demographics of $S_{A=1}^t$ of a 10-site Ising chain of (17) near an integrable point when comparing with the corresponding GGE state specified by the chemical potentials (β_0, β_1) of the conserved charges (20). The phase diagram of the Ising chain is shown in the inset of the bottom subfigure, on which a redline is a region we plot for thermalization demographics. The integrable point on the redline is $h_x = 1.05$ and $h_z = 0$. We plot 10 demographics from $h_z = 0$ to $h_z = 0.1$. At the integrable point, the GGE state is just a p-GGE one, as all the conserved charges other than Q_1 are ignored. The results show that the thermalization hypothesis breaks down badly near the integrable point but gradually holds better as moving away from the integrable point.

long enough to ensure the typicality. Based on this, we will prepare the typical states by choosing $T = 1000$.

III. THERMALIZATION DEMOGRAPHICS FOR QUANTUM ISING SPIN CHAINS

As a starter, we consider the quantum Ising spin chain in the transverse field h_x and longitudinal field h_z , given by the Hamiltonian

$$H = \sum_{i=1}^L (h_x \sigma_i^x + h_z \sigma_i^z + \sigma_i^z \sigma_{i+1}^z), \quad (17)$$

where σ_i^x, σ_i^z are Pauli matrix operator on the site i , and L is the number of spins. This model possesses a Z_2 reflection symmetry Π , which swaps the order of spins by sending site i to $L + 1 - i$, i.e.,

$$\Pi := \begin{cases} P_{1,L} P_{2,L-2} \cdots P_{\frac{L}{2}, \frac{L+2}{2}} & \text{if } L = \text{is even} \\ P_{1,L} P_{2,L-2} \cdots P_{\frac{L-1}{2}, \frac{L+3}{2}} & \text{if } L = \text{is odd} \end{cases} \quad (18)$$

where $P_{k,l} = (\sigma_k^x \sigma_l^x + \sigma_k^y \sigma_l^y + \sigma_k^z \sigma_l^z + I)/2$ is the permutation operator and I is the identity operator. $P_{k,l}$ can swap the state of k^{th} and l^{th} sites.

This model is integrable if $h_x = 0$ or $h_z = 0$. Otherwise, it is nonintegrable. Its phase diagram is shown in the inset of the bottom subfigure of Fig. 3, e.g., see [35]. It was shown that the level-spacing statistics of the superselection sectors

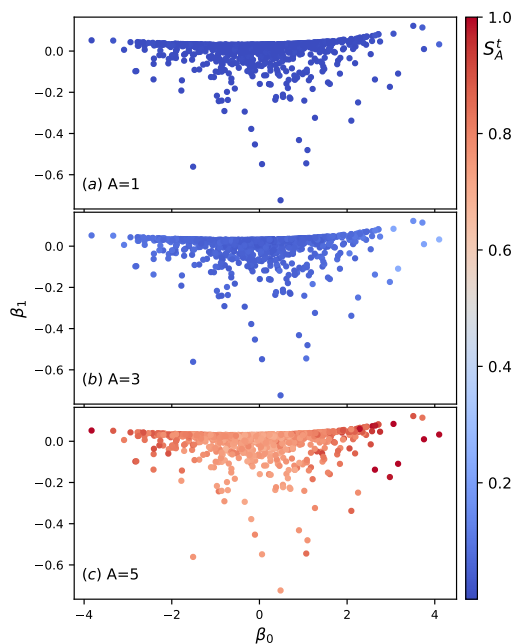


FIG. 4. Density plots of typical-state thermalization demographics: $S_{A=1,3,5}^t$ v.s. (β_0, β_1) of a GGE state for the Ising chain of (19) with conserved charges $Q_{0,1}$ given by (20). The thermalization hypothesis works well for $A = 1$ in subfigure (a) and worsens as A increases, i.e., for $A = 3$ in subfigure (b) and $A = 5$ in subfigure (c).

with $\Pi = \pm 1$ match with the Wigner-Dyson distribution for the nonintegrable Ising chain [31]. Despite that, we can examine how the pattern of the demographics of S_A^t changes by tuning the coupling constant to make the model more nonintegrable. The thermalization hypothesis holds well if most of the population lives near $S_A^t = 0$. Otherwise, we can quantify the violation of the thermalization hypothesis by the spreading of the population away from $S_A^t = 0$. A typical result for such pattern changes is shown in Fig. 3. We see that the demographics of S_1^t for the integrable case violate the subsystem thermalization hypothesis badly. However, as the model moves away from the integrable point, the values of S_1^t gradually converge to zero.

From now on, we will focus on the nonintegrable Ising chains, specifically for the model with the following parameters:

$$L = 10, \quad h_x = 1.05, \quad h_z = 0.5. \quad (19)$$

This model has two conserved charges denoted by

$$Q_0 = H, \quad Q_1 = \Pi. \quad (20)$$

We will present $S_A^{t,a,e}$ demographics for various kinds of p-GGE states.

A. Demographics of typical-state thermalization

We first consider the subsystem thermalization hypothesis for the typical states. In Fig. 4, we show the thermalization

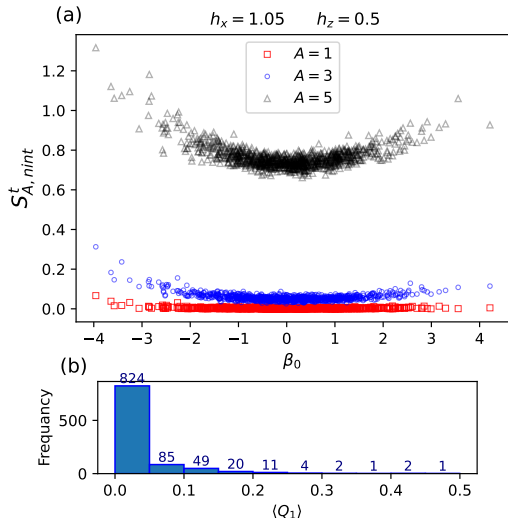


FIG. 5. (a) Typical-state thermalization demographics: $S_{A=1,3,5}^t$ v.s. β_0 for the Ising chain of (19) by comparing with a p-GGE specified only by β_0 . The thermalization hypothesis also works well for $A = 1$ (red squares), but it worsens as A increases, i.e., $A = 3$ (blue circles) and $A = 5$ (black triangles). (b) Demographics of the typical states classified by the $\langle Q_1 \rangle$.

demographics of the relative entropy S_A^t of the region A with 1, 3, 5 sites (denoted by $A = 1, 3, 5$) between a typical state and the corresponding GGE specified by (β_0, β_1) . Since the GGE contains two chemical potential parameters β_0 and β_1 , thus we present the demographics in the form of density plots. For $A = 1$, S_A^t 's of all the typical states considered are almost

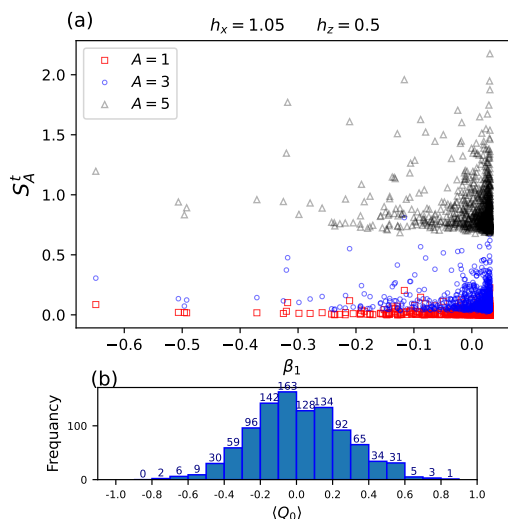


FIG. 6. (a) Typical-state thermalization demographics: $S_{A=1,3,5}^t$ v.s. β_1 for the Ising chain of (19) by comparing with a p-GGE specified only by β_1 . Again, the thermalization hypothesis works well for $A = 1$ and worsens as A increases. (b) Demographics of the typical states classified by the $\langle Q_0 \rangle$.

vanishing. This implies that the thermalization hypothesis for the typical states works well for $A = 1$ when compared with the corresponding GGE thermal states. On the other hand, for $A = 3$, the thermalization hypothesis still looks good, with some exceptions for large $|\beta_0|$ or $|\beta_1|$. However, when $A = 5$, the thermalization hypothesis breaks down. The above patterns of dependence of validity of the thermalization hypothesis on the size A are expected and also give the explicitly quantitative picture.

Besides checking the typical-state thermalization hypothesis, Fig. 4 also reveals the demographics of the typical states on the (β_0, β_1) of the corresponding GGE ensemble states. Interestingly, the inverse temperature β_0 can be either positive or negative and almost symmetric about $\beta_0 = 0$. The GGE states with negative (inverse) temperatures are hypothetical and cannot be realized naturally. However, we see that they can be realized by typical states. Moreover, the thermalization hypothesis works even for such hypothetical GGE thermal ensemble states. On the other hand, the chemical potential β_1 for reflection symmetry Π is almost negative for the typical states we construct. It is unclear why there is such a bias.

After considering the comparison with GGE states, we now compare with the corresponding p-GGE thermal states. In Fig. 5, we present the typical-state demographics of S_A^t when compared with the corresponding p-GGE states specified only by β_0 (inverse temperature). On the other hand, in Fig. 6, we compare the typical states with the corresponding p-GGE states specified only by β_1 . We see that the features of demographics of p-GGE on either β_0 , i.e., symmetric about β_0 , and β_1 , i.e., favors negative values, are the same as the ones of GGE. Regarding the validity of the typical-state thermalization hypothesis, we see in both Fig. 5 and 6 the similar patterns of dependence on the size A as in Fig. 4 for GGE states's comparison. In all three cases, the thermalization hypothesis for the typical states works quite well for $A = 1$ and gradually worsens with increasing A .

Although it is generally believed that the typical-state thermalization hypothesis will hold for small subsystems, we shall emphasize that it is unclear if it will hold for various thermal ensemble states and how local the subsystem should be for it to hold. Our results presented here have clarified these issues.

B. Demographics of almost superselection-state thermalization

We now consider the thermalization hypothesis for the almost superselection states. This is to subdivide the typical states into the almost superselection sectors specified by $\langle Q_a \rangle$. This is a fine-grained version of the typical-state thermalization hypothesis considered above. We take snapshots of the population demographics of S_A^a with different values of $\langle Q_a \rangle$ to see how the thermalization hypothesis works at the fine-grained level. Recall the validity of the typical-state thermalization hypothesis shown in Fig. 5 and 6 when compared with p-GGE specified by β_0 and β_1 , we now examine their fine-grained counterparts to see if the thermalization hypothesis also holds well for each almost superselection sector.

In Fig. 7, we consider the almost superselection typical

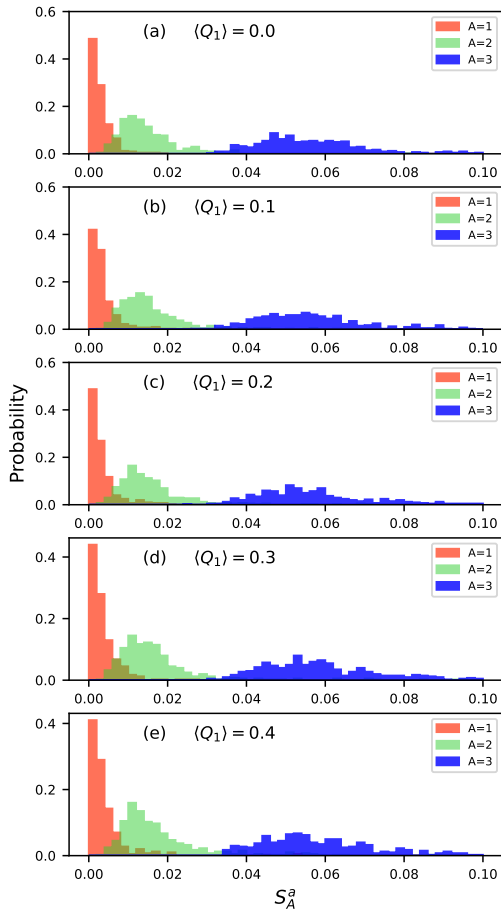


FIG. 7. Fine-grained version of Fig. 5 as the corresponding almost-superselction-state thermalization demographics by showing the population ratios for the collection of typical states with fixed $\langle Q_1 \rangle =$ (a) 0.0, (b) 0.1, (c) 0.2, (d) 0.3, and (e) 0.4, respectively. The thermalization hypothesis works well for $A = 1$ (blue) but not so for $A = 2$ (red) and $A = 3$ (green).

states with fixed $\langle Q_1 \rangle$ and compare them with the corresponding p-GGE states specified by β_0 . In Fig. 8, we swap the role of the Q_0 and Q_1 , that is, compare the almost superselction states with fixed $\langle Q_0 \rangle$ to the corresponding p-GGE states specified by β_1 . In both cases, we show the population ratio demographics against S_A^a . The population ratio for a given $\langle Q_a \rangle$ is defined with respect to the total number of all typical states considered. We can quantify the violation of the thermalization hypothesis by the spreading of the population away from $S_A^a = 0$. In the first case, as shown in Fig. 7, the thermalization hypothesis holds well for each almost superselction sector if $A = 1$. Moreover, the patterns of the populations for different A 's do not change much as $\langle Q_1 \rangle$ varies. In the second case, as shown in Fig. 8, the thermalization holds well only for $\langle Q_0 \rangle = 0$ and worsens more and more as $\langle Q_0 \rangle = 0$ increases even for $A = 1$. In this case, even the typical-state thermalization holds, but its fine-grained version does not. Unlike in Fig. 7, the patterns of populations for different A 's change more significantly as $\langle Q_0 \rangle$ varies.

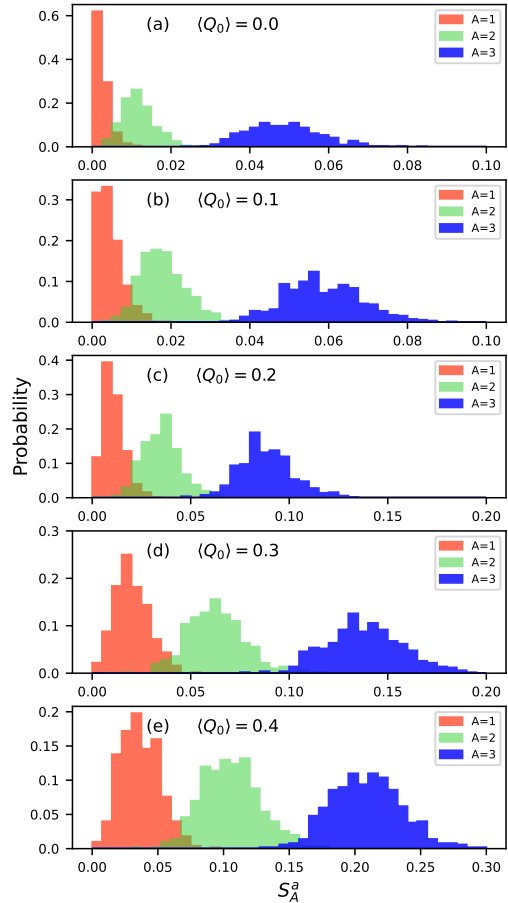


FIG. 8. Fine-grained version of Fig. 6 as the corresponding almost-superselction-state thermalization demographics by showing the population ratios for the collection of typical states with fixed $\langle Q_0 \rangle =$ (a) 0.0, (b) 0.1, (c) 0.2, (d) 0.3, and (e) 0.4, respectively. Unlike Fig. 7, the thermalization hypothesis does not work well even for $A = 1$ when $\langle Q_0 \rangle$ increases away from zero. However, the sector of $\langle Q_0 \rangle = 0$ has the largest population as shown in Fig. 6(b), so the corresponding coarse-grained thermalization in Fig. 6 looks fine.

It may look strange why the coarse-grained version of the thermalization hypothesis holds, but most of its fined-grained versions fail. However, if we look into the scales of the population ratio in each subfigure, it can be understood that the population respecting the thermalization hypothesis dominates; see also Fig. 6(b), where the sector of $\langle Q_0 \rangle = 0$, which obeys the thermalization hypothesis as shown in the first subfigure of Fig. 8, has the largest population.

In summary, when comparing the typical states with some chosen thermal ensemble states, the fine-grained version of the thermalization hypothesis may fail even when the coarse-grained one holds.

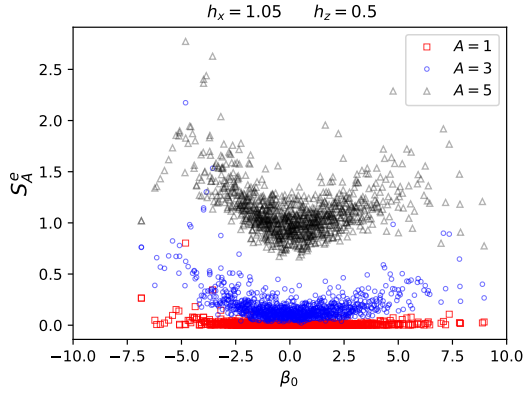


FIG. 9. Subsystem eigenstate thermalization demographics: $S_{A=1,3,5}^e$ v.s. β_0 for the Ising chain of (19) by comparing with a p-GGE specified only by β_0 . The thermalization hypothesis also works well for $A = 1$ (red squares), but it worsens as A increases, i.e., $A = 3$ (blue circles) and $A = 5$ (black triangles).

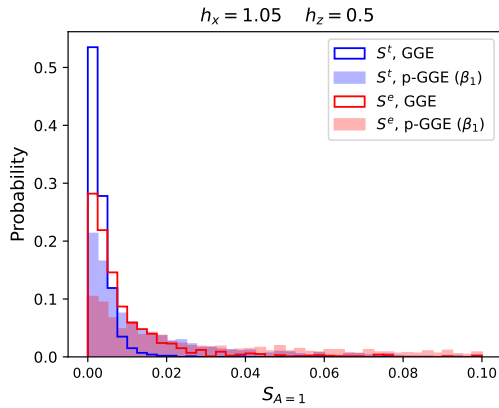


FIG. 10. Subsystem eigenstate thermalization demographics of $S_{A=1}^e$ for the Ising chain of (19) by comparing with (i) GGE states (empty red) and (ii) p-GGE states specified by β_1 (solid pink). We also present the typical-state counterparts (empty blue and solid gray) for comparison. The subsystem thermalization hypothesis works better for GGE than p-GGE, and better for typical states than eigenstates.

C. Demographics of eigenstate thermalization

We finally consider the subsystem ETH [10–12], which has been extensively studied for integrable (1 + 1)-dimensional conformal field theories [12, 17–24]. Here, we will consider the subsystem ETH for the non-integrable Ising chains. Since the conserved charge Π commutes with the Hamiltonian H , thus the eigenstates are also the superselection states. As in the usual case for subsystem ETH, we first consider the demographics S_A^e when comparing with the canonical ensemble thermal state, i.e., p-GGE specified by β_0 , and the result is shown in Fig.9. We see the subsystem ETH holds well for $A = 1$ and worsens as A increases. We expect this A -

dependence will be similar when considering the GGE or the other p-GGE. Thus, we now only consider the demographics of the subsystem ETH for only $A = 1$. The demographics for GGE specified by (β_0, β_1) and p-GGE by β_1 are shown in Fig.10, in which we also compare with their counterparts of typical-state thermalization hypothesis. Interestingly, for both eigenstates and typical states, the subsystem thermalization hypothesis works better for the GGE than the p-GGE specified by β_1 . On the other hand, the subsystem thermalization hypothesis works better for the typical states than the eigenstates for a chosen type of thermal ensemble state. Our results verify the subsystem ETH in a broader context than the canonical ensemble and also show an interesting comparison with the typical-state thermalization hypothesis.

IV. THERMALIZATION DEMOGRAPHICS OF QUANTUM SPIN-1/2 XXZ CHAINS WITH $U(1)$ SYMMETRY

To consider spin chains with more rich symmetries, such as non-Abelian ones, we consider the following L -site spin-1/2 XXZ spin chain model with the following Hamiltonian [36]

$$\begin{aligned}
 H = & J \sum_{i=1}^L (S_i^x S_{i+1}^x + S_i^y S_{i+1}^y + \Delta S_i^z S_{i+1}^z) \\
 & + \lambda J \sum_{i=1}^L (S_i^x S_{i+2}^x + S_i^y S_{i+2}^y + \Delta S_i^z S_{i+2}^z) \\
 & + dJ S_{L/2}^z + \sum_{i=1}^L h_i J S_i^z, \quad (21)
 \end{aligned}$$

where $\vec{S}_i := \vec{\sigma}_i/2$ is the spin vector operator at the i -th site. Besides, the parameter dJ denotes the Zeeman splitting at the defect site. The Zeeman splitting $h_i J$ reflects onsite disorder due to random static magnetic fields, with h_i being random values drawn from a uniform distribution within $[-h, h]$, where h indicates the disorder strength. The anisotropy parameter Δ determines the interaction type: the system is isotropic when $\Delta = 1$, meaning the Ising interaction and the flip-flop term are of equal strength. The parameter λ characterizes the relative size of the nearest-neighbor (NN) coupling to the next-nearest-neighbor (NNN) coupling.

The symmetry properties of this model can be summarized as follows [36]:

- (i) H commutes with $S_{\text{tot}}^z := \sum_{k=1}^L S_k^z$.
- (ii) This model is integrable if $d = h = \lambda = 0$. If $\Delta = 0$, it reduces to a non-interacting XX model.
- (iii) H is invariant under reflection Π as in quantum Ising chain, if $d = h = 0$.
- (iv) H commutes with $\vec{S}_{\text{tot}} := \sum_{k=1}^L \vec{S}_k$ if $d = h = 0$ and $\Delta = 1$. This special model with non-Abelian $SU(2)$ symmetry is called the XXX model.
- (v) H is invariant under a global π -rotation around the x -axis, i.e., $R_\pi^x = \sigma_1^x \sigma_2^x \cdots \sigma_L^x$, if $d = h = 0$, L is even and the number of up spins in the z -direction $N_{\text{up}} = L/2$.

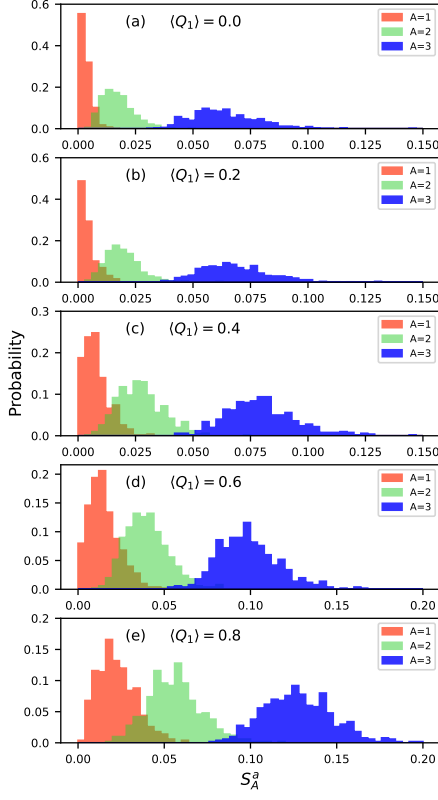


FIG. 11. Thermalization demographics of population ratios of S_A^a for the XXZ chain of (22) with $U(1)$ conserved charge for p-GGE specified only by β_0 for various almost-superselction states with fixed $\langle Q_1 \rangle =$ (a) 0.0, (b) 0.2, (c) 0.4, (d) 0.6, and (e) 0.8, respectively. This is the fine-grained version of Fig. 22 of Appendix A. The thermalization hypothesis does not work well even for $A = 1$ when $\langle Q_1 \rangle$ increases away from zero.

- (vi) This model is chaotic if the NNN coupling $0 < \lambda < 1$ and $h = 0$ (no random disorder) for both XXZ ($\Delta \neq 0$) and XX ($\Delta = 0$) models. This can be verified by fitting the level spacing statics to the Wigner-Dyson distribution, as shown in Fig. 19 of Appendix A.

We will consider only the non-integrable cases. This section will focus on the XXZ chain with only S_a as the $U(1)$ conserved charge. Specifically, we will consider the Hamiltonian (21) with

$$L = 10, \quad \Delta = \lambda = 0.5, \quad h = d = 0, \quad J = 1. \quad (22)$$

We consider the two conserved charges of this model denoted by

$$Q_0 = H, \quad Q_1 = S_{\text{tot}}^z. \quad (23)$$

In the next section, we will consider the XXX model with \vec{S}_{tot} as the $SU(2)$ conserved charges. Since we have studied the subsystem thermalization hypothesis for the Ising chain with Π as the Z_2 conserved charge, we will ignore this discrete charge for the following considerations.

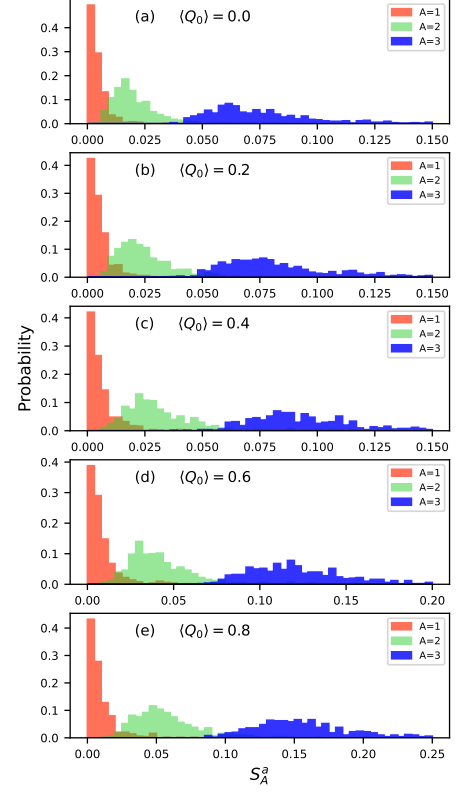


FIG. 12. Thermalization demographics of the population ratios of S_A^a for the XXZ chain of (22) with $U(1)$ conserved charge for p-GGE specified only by β_1 for various almost-superselction states with fixed $\langle Q_0 \rangle =$ (a) 0.0, (b) 0.2, (c) 0.4, (d) 0.6, and (e) 0.8, respectively. This is the fine-grained version of Fig. 21 of Appendix A. The thermalization hypothesis works well for $A = 1$ (blue) but not so for $A = 2$ (red) and $A = 3$ (green).

As in the cases of quantum Ising chains, we consider the demographics of relative entropies $S_A^{t,a,e}$ for both GGE and p-GGEs. The demographics of S_A^t bear similar patterns as in the Ising cases; that is, the subsystem thermalization hypothesis holds well for $A = 1$ and worsens as A increases. Thus, we will not show the results in the main text but in Appendix A.

As for the thermalization demographics of S_A^a , we find something interesting when compared with the Ising counterparts. In the Ising case, the subsystem thermalization hypothesis works well for $A = 1$ for all fixed values of $\langle Q_1 \rangle$, but only for small values of $\langle Q_0 \rangle$. However, as shown in Fig. 11 and 12, we see the role of Q_0 and Q_1 swap, that is, the subsystem thermalization hypothesis works well for $A = 1$ for all fixed values of $\langle Q_0 \rangle$, but only for small values of $\langle Q_1 \rangle$.

Finally, we consider the subsystem ETH for the XXZ chains. With loss of generality, we only compare with the GGE states specified by (β_0, β_1) . The result is shown in Fig. 13. We see the subsystem ETH holds well for $A = 1$ but worsens as A increases. Also, the plot patterns for the XXZ chain of $U(1)$ charges differ from the Ising ones with Z_2 charges.

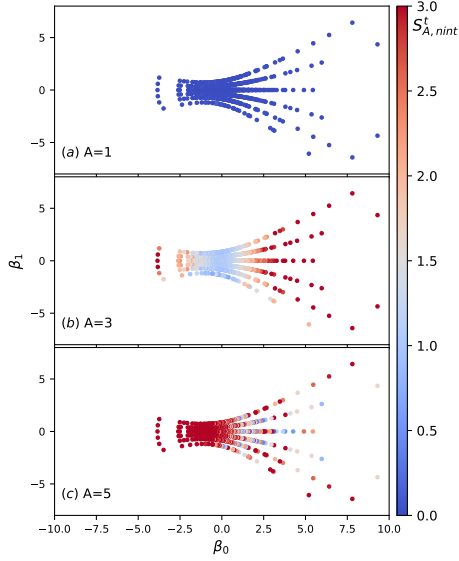


FIG. 13. Density plot for the subsystem ETH: demographics of S_A^e of the XXZ chain of (22) with $U(1)$ conserved charge for GGE specified by (β_0, β_1) . The subsystem ETH works well for $A = 1$ but worsens as A increases.

V. THERMALIZATION DEMOGRAPHICS OF QUANTUM SPIN-1/2 XXZ CHAINS WITH $SU(2)$ SYMMETRY

We now will consider the thermalization demographics for the nonintegrable XXX chains with $SU(2)$ conserved charges. Specifically, we will consider the Hamiltonian of (21) with

$$L = 10, \quad \Delta = J = 1, \quad \lambda = 0.5, \quad d = h = 0. \quad (24)$$

We consider the four conserved charges denoted as follows:

$$Q_0 = H, \quad Q_1 = S_{\text{tot}}^x, \quad Q_2 = S_{\text{tot}}^y, \quad Q_3 = S_{\text{tot}}^z. \quad (25)$$

The charges $Q_{1,2,3}$ do not commute among themselves. Thus, we can only specify the eigenstates by Q_0 and one of Q_i with $i = 1, 2, 3$. As usual, we will specify the eigenstates by (Q_0, Q_3) . On the other hand, we can further classify the typical states into the almost superselection sectors with fixed values of $\langle Q_{\mu=0,1,2,3} \rangle$. We will consider the subsystem thermalization hypothesis for typical states and energy eigenstates by comparing them locally with GGE states and various types of p-GGE states. Note that the GGE states

$$\rho_{\text{GGE}}^{\text{SU}(2)} = \frac{e^{-\sum_{\mu=0}^3 \beta_{\mu} Q_{\mu}}}{Z}, \quad Z := \text{Tr} e^{-\sum_{\mu=0}^3 \beta_{\mu} Q_{\mu}} \quad (26)$$

are proposed and studied in [26–29] for the ETH of the system with non-commuting conserved charges, and called non-Abelian thermal states (NATS).

A. Demographics of typical-state thermalization

We first consider the subsystem thermalization hypothesis for the typical states compared to GGE states (or NATS), spec-

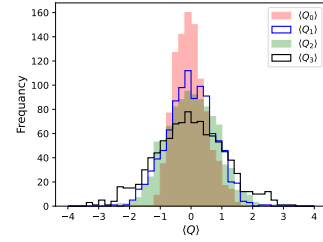
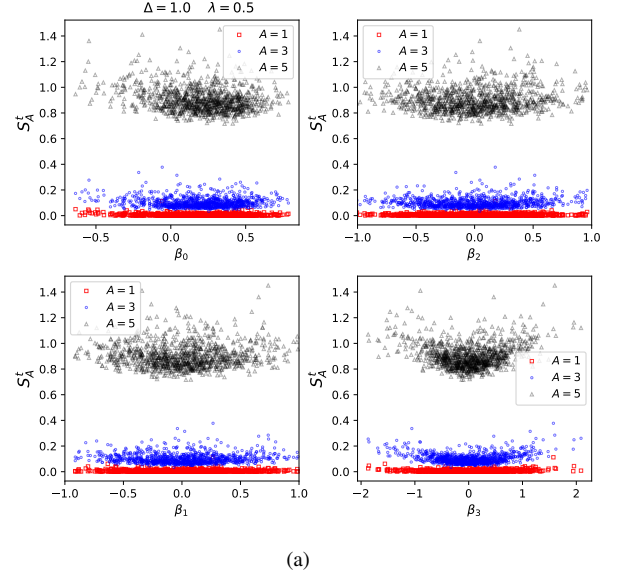


FIG. 14. Demographics of typical-state thermalization hypothesis for the XXX chain of (24) by comparing with the GGE states specified by $\beta_{\mu=0,1,2,3}$, which are the chemical potentials of the conserved charged defined in (25). (a) Density plots of $S_{A=1,3,5}^t$ v.s. $\beta_0, \beta_1, \beta_2$, and β_3 . The subsystem thermalization hypothesis holds well for $A = 1$ and worsens as A increases. (b) Demographics of the typical states classified by the $\langle Q_0 \rangle$ (solid pink), $\langle Q_1 \rangle$ (empty blue), $\langle Q_2 \rangle$ (solid green), and $\langle Q_3 \rangle$ (empty black).

ified by the chemical potentials $\beta_{\mu=0,1,2,3}$. It is impossible to simultaneously express the demographics of S_A^t of four chemical potentials. Instead, we look into the dependence of each chemical potential of the full demographics. The results are shown in Fig. 14, in which we also show the demographics of $\langle Q_{\mu=0,1,2,3} \rangle$ of the typical states. Again, the subsystem thermalization holds well for $A = 1$ and worsens as A increases. Our result confirms that NATS/GGE states can be adopted for the thermalization hypothesis of the typical states even though the conserved charges are noncommuting².

² Our result, in fact, confirms the non-Abelian ETH proposed in [26] based on the subsystem version of the thermalization hypothesis for typical states. This is because the ETH considered in [26] is examined by comparing the time average of the expectation values of the local observables on the evolved pure states with the corresponding thermal average over the

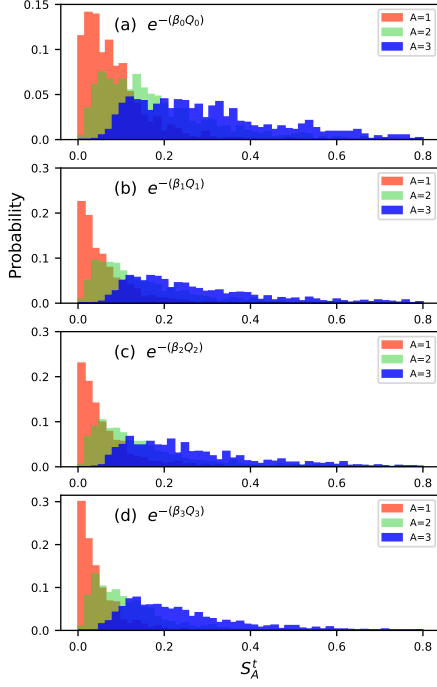


FIG. 15. Typical-state thermalization demographics of the population ratios of $S_{A=1,2,3}^t$ for the XXX chain of (24) for the p-GGE of a single charge: (a) $S_{A=1,2,3}^t$ v.s. β_0 , (b) $S_{A=1,2,3}^t$ v.s. β_1 , (c) $S_{A=1,2,3}^t$ v.s. β_2 , and (d) $S_{A=1,2,3}^t$ v.s. β_3 .

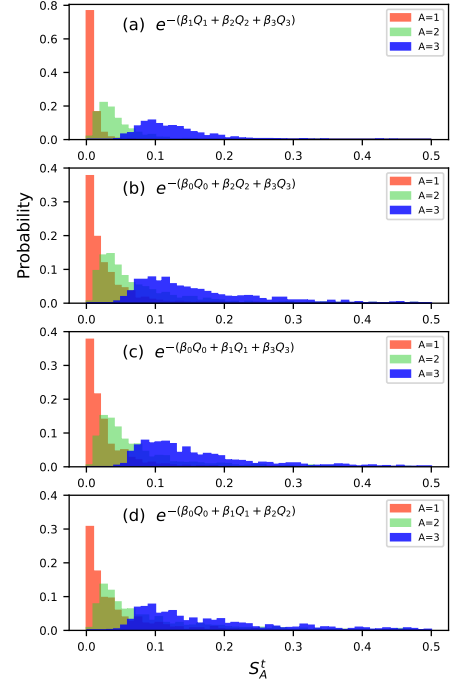


FIG. 17. Typical-state thermalization demographics of the population ratios of $S_{A=1,2,3}^t$ for the XXX chain of (24) for the p-GGE of three charges: (a) $S_{A=1,2,3}^t$ v.s. $(\beta_1, \beta_2, \beta_3)$, (b) $S_{A=1,2,3}^t$ v.s. $(\beta_0, \beta_2, \beta_3)$, (c) $S_{A=1,2,3}^t$ v.s. $(\beta_0, \beta_1, \beta_3)$, and (d) $S_{A=1,2,3}^t$ v.s. $(\beta_0, \beta_1, \beta_2)$.

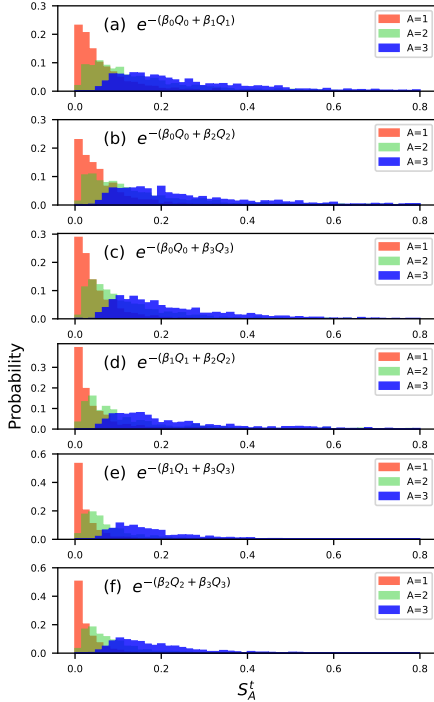


FIG. 16. Typical-state thermalization demographics of the population ratios of $S_{A=1,2,3}^t$ for the XXX chain of (24) for the p-GGE of two charges: (a) $S_{A=1,2,3}^t$ v.s. (β_0, β_1) , (b) $S_{A=1,2,3}^t$ v.s. (β_0, β_2) , (c) $S_{A=1,2,3}^t$ v.s. (β_0, β_3) , (d) $S_{A=1,2,3}^t$ v.s. (β_1, β_2) , (e) $S_{A=1,2,3}^t$ v.s. (β_1, β_3) , and (f) $S_{A=1,2,3}^t$ v.s. (β_2, β_3) .

We now move to the p-GGEs. To demonstrate the richness of the p-GGEs, we first consider the subsystem thermalization hypothesis by comparing the typical states with the p-GGE states with (i) single conserved charges, (ii) two conserved charges, and (iii) three conserved charges. The results are presented in Fig. 15, 16 and 17, respectively. The overall features of these results are as follows. First, the subsystem thermalization hypothesis works better for the p-GGEs with more conserved charges. Second, for the p-GGEs of the same number of charges, the subsystem thermalization hypothesis works better for the ones involving no Q_0 . Thus, if we restrict to $A = 1$, our results suggest that the typical-state thermalization hypothesis holds quite generically for the p-GGEs with at least two conserved charges without involving Q_0 . This implies that NATs are not the only thermal ensemble states adopted for the subsystem thermalization hypothesis for the typical states. Indeed, our framework with p-GGEs extends the thermalization hypothesis to a more general scope. In particular, it is quite interesting to see that the thermalization hypothesis also works for those p-GGEs with $Q_0 = H$ excluded. This implies that the Hamiltonian may not be essential for considering quantum thermalization. This is also implied by the fact that the (inverse) temperatures for some of

NATs/GGE ensemble states. The former ones are equivalent to the average of the expectation values of the local observables on the typical states.

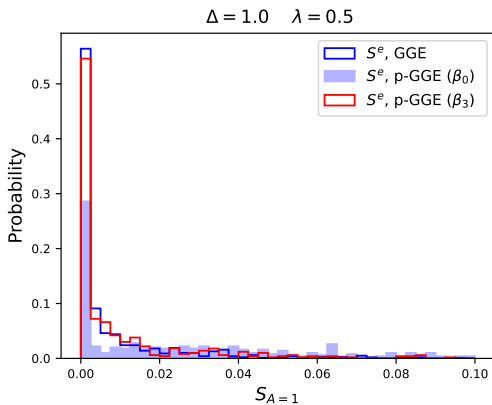


FIG. 18. Subsystem eigenstate thermalization demographics of $S_{A=1}^e$ for the XXX chain of (24) by comparing with (i) GGE states (empty blue) and (ii) p-GGE states specified by β_0 (solid blue) and (iii) p-GGE states specified by β_3 (empty red). The subsystem thermalization hypothesis works better for GGE than p-GGE.

the corresponding GGE or p-GGE are negative, which bears no physical meaning in realistic thermodynamics. This could be related to the thermalization hypothesis working better for the p-GGEs without Q_0 than those with Q_0 .

B. Demographics of eigenstate thermalization

Finally, we consider the subsystem ETH for the XXX chains with $SU(2)$ conserved charges. Since the $SU(2)$ charges are noncommuting, we choose the eigenstates to be specified by the energy E and the z -component of the total spin, i.e., S_{tot}^z . For such eigenstates, the expectation values of S_{tot}^x and S_{tot}^y vanishes, as expected by the usual argument for the Stern-Gerlach experiment. Thus, it is only sensible to consider subsystem ETH with the p-GGEs specified by either β_0 or β_3 or the GGE specified by both. As usual, the subsystem thermalization hypothesis holds well for $A = 1$ and worsens as A increases. Thus, we only show the demographics of $S_{A=1}^e$ in Fig. 18. The results show that the subsystem ETH works almost equally well for GGE and p-GGE specified by β_3 , both better than the p-GGE specified by β_0 . This is similar to the previous cases for typical states and for the XXZ chain.

VI. CONCLUSION

Quantum thermalization is fascinating because it yields deep implications for the second-law perspective of pure states. Compared to the thermalization for the open quantum system or classical system, quantum thermalization can manifest even without taking the thermodynamic limit. This implies that we can implement the exact diagonalization method to examine the thermalization hypothesis of a not-so-large system as long as the subsystem size is small enough com-

pared to the system size. This provides the starting point for the numerical plots done in this work. The usual considerations for the thermalization hypothesis are done for the systems without conserved charges so that the corresponding thermal ensemble for comparison is either the micro-canonical or canonical ensemble. This work extensively considers the subsystem thermalization hypothesis of the typical states or eigenstates for the systems with conserved charges of Z_2 , $U(1)$ or $SU(2)$ symmetries. Furthermore, we generalize the thermal ensembles beyond the generalized Gibbs ensemble (GGE). We call these thermal ensembles the partial-GGE (p-GGE), of which some conserved charges are excluded. Moreover, in the framework of p-GGEs, the Hamiltonian and other conserved charges are treated on equal footing. Moreover, our results show that the p-GGEs with H excluded usually yield better results for quantum thermalization than the ones with H .

Based on the framework of the subsystem thermalization hypothesis with p-GGEs, we can quantify the validity of this scheme by the smallness of the relative entropy between the subsystem's reduced states obtained from the typical states/eigenstates and the corresponding p-GGEs. We can then examine the universality of quantum thermalization with various p-GGEs by numerically calculating the demographics of relative entropies. Our results of thermalization demographics demonstrate that the subsystem thermalization hypothesis of the typical states (and their fine-grained versions) and eigenstates compared to p-GGEs holds well quite generically as long as the subsystem size is small enough. However, there are some cases where the subsystem typical-state thermalization hypothesis fails, for example, for the p-GGEs of $SU(2)$ case with one or two conserved charges, especially with the Hamiltonian included. Despite that, our results show that the thermalization hypothesis can be extended to p-GGEs even without including Hamiltonian. This greatly enlarges the scope of quantum thermalization and will deserve future studies for more general systems with conserved charges and larger sizes.

ACKNOWLEDGMENTS

FLL and JJH are supported by Taiwan's NSTC with Grant No. 109-2112-M-003-007-MY3 and 112-2112-M-003-006-MY3. CYH is supported by Taiwan's National Science and Technology Council (NSTC) with Grant No. 113-2112-M-029-002-.

Appendix A: Typical-state thermalization demographics of the XXZ chain with $U(1)$ conserved charges

As mentioned in the main text, This model is chaotic if the NNN coupling $0 < \lambda < 1$ and $h = 0$ (no random disorder) for both XXZ ($\Delta \neq 0$) and XX ($\Delta = 0$) models. We verify this by fitting the level spacing statistics to the Wigner-Dyson distribution, as shown in Fig. 19. This is consistent with the thermalization hypothesis. For readers' interest, we

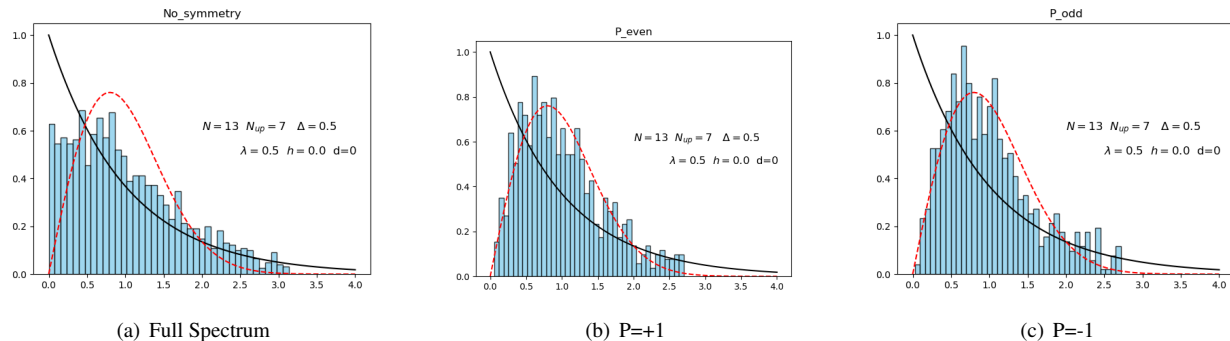


FIG. 19. Level spacing demographics of energy and parity eigenstates for a $L = 13$ quantum XXZ open chain for (a) full spectrum, (b) even-parity spectrum, and (c) odd-parity spectrum. The XXZ chain considered is described by (21) with $N_{up} = 7$, $d = h = 0$, $\Delta = \lambda = 0.5$ and $J = 1$. This model is non-integrable and has a $U(1)$ symmetry of S_{tot}^z and a parity symmetry of the π -rotation symmetry around the x-axis. We show that the level-spacing distributions for spectra of superselection sectors fit the Wigner-Dyson distribution (red dashed curve) but not the Poisson distribution (solid black curve) to which the one of the full spectrum is closer. This is consistent with the expectation of the thermalization hypothesis.

also present the density plots of three quantities to characterize the GGE thermal states associated with the same numerically model considered in Fig. 19.

We now consider the demographics of the thermalization hypothesis. As we have presented the plots for $S_A^{a,e}$ in the main text, we will only show the ones for the typical states. Although we consider the $U(1)$ charge, not the Z_2 of this XXZ model for the GGE or p-GGE states, the typical-state thermalization demographics bear similar patterns and features as in the Ising case with only Z_Z conserved charge. The XXZ model we consider is described by the Hamiltonian (21) with the coupling parameters given by $L = 10$, $\Delta = \lambda = 0.5$, $h = d = 0$, and $J = 1$. The demographics for GGE specified by (β_0, β_1) , and p-GGE specified by β_0 and β_1 are given in the Fig. 20, 21 and 22, respectively. The thermalization hypothesis seems to work better in Fig. 22 than in Fig. 21.

The result shows that the subsystem typical-state thermal-

ization hypothesis works well for $A = 1$ and worsens as A increases, as in the Ising cases. Despite that, it is interesting to compare the demographic patterns of Fig. 20 with its Ising counterpart shown in Fig. 4. We see that the current patterns are more uniform on the (β_0, β_1) -plane due to the continuous symmetry instead of the discrete one.

The fine-grained versions of Fig. 21 and Fig. 22 as the corresponding almost-superselection-state thermalization demographics shown in Fig. 12 and Fig. 11, respectively. We see that the almost-superselection-state thermalization hypothesis for $A = 1$ works well for the p-GGE specified by β_1 , not for the p-GGE specified by β_0 for which the thermalization hypothesis worsens as $\langle Q_1 \rangle$ increases away from zero. Interestingly, the almost-superselection-state thermalization demographics of quantum Ising chains, as shown in Fig. 7 and 8, works for the p-GGE specified by β_0 , but not for the p-GGE specified by β_1 . It is the opposite for the ZZ chains.

-
- [1] J. von Neumann, Proof of the ergodic theorem and the h-theorem in quantum mechanics, *The European Physical Journal H* **35**, 201 (2010).
- [2] J. M. Deutsch, Quantum statistical mechanics in a closed system, *Phys. Rev. A* **43**, 2046 (1991).
- [3] M. Srednicki, Chaos and Quantum Thermalization, *Phys. Rev. E* **50** (1994), arXiv:cond-mat/9403051.
- [4] M. Srednicki, Thermal fluctuations in quantized chaotic systems, *J. Phys. A* **29**, L75 (1996), arXiv:chao-dyn/9511001.
- [5] M. Rigol, V. Dunjko, and M. Olshanii, Thermalization and its mechanism for generic isolated quantum systems, *Nature* **452**, 854 (2007).
- [6] L. D'Alessio, Y. Kafri, A. Polkovnikov, and M. Rigol, From quantum chaos and eigenstate thermalization to statistical mechanics and thermodynamics, *Adv. Phys.* **65**, 239 (2016), arXiv:1509.06411 [cond-mat.stat-mech].
- [7] C. Gogolin and J. Eisert, Equilibration, thermalisation, and the emergence of statistical mechanics in closed quantum systems, *Rept. Prog. Phys.* **79**, 056001 (2016), arXiv:1503.07538 [quant-ph].
- [8] T. Mori, T. N. Ikeda, E. Kaminishi, and M. Ueda, Thermalization and prethermalization in isolated quantum systems: a theoretical overview, *J. Phys. B* **51**, 112001 (2018), arXiv:1712.08790 [cond-mat.stat-mech].
- [9] J. M. Deutsch, Eigenstate thermalization hypothesis, *Reports on Progress in Physics* **81** (2018).
- [10] A. Dymarsky, N. Lashkari, and H. Liu, Subsystem ETH, *Phys. Rev. E* **97**, 012140 (2018), arXiv:1611.08764 [cond-mat.stat-mech].
- [11] N. Lashkari, A. Dymarsky, and H. Liu, Eigenstate Thermalization Hypothesis in Conformal Field Theory, *J. Stat. Mech.* **1803**, 033101 (2018), arXiv:1610.00302 [hep-th].
- [12] S. He, F.-L. Lin, and J.-j. Zhang, Subsystem eigenstate thermalization hypothesis for entanglement entropy in CFT, *Journal of High Energy Physics* **08**, 126 (2017), arXiv:1703.08724 [hep-th].

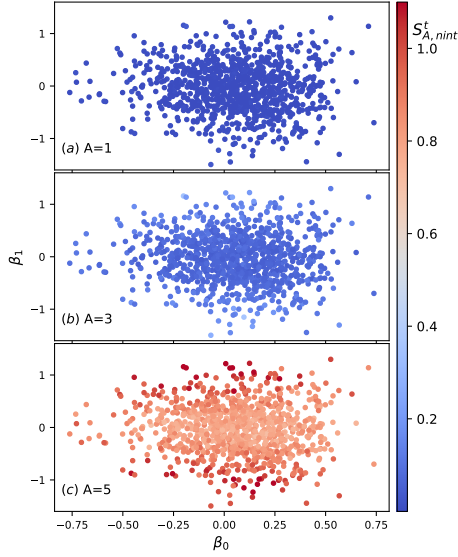


FIG. 20. Density plots of typical-state thermalization demographics: $S_{A=1,3,5}^t$ v.s. (β_0, β_1) for the XXZ chain of (22) when comparing with the GGE states specified by (β_0, β_1) , i.e., respectively the inverse temperature and the chemical potential to the $Q_1 = S_{\text{tot}}^z$. The thermalization hypothesis works well for $A = 1$ (a) and worsens as A increases, i.e., for $A = 3$ (b) and $A = 5$ (c).

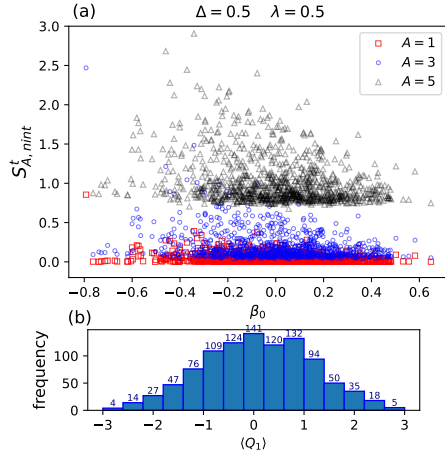


FIG. 21. (a) Typical-state thermalization demographics: $S_{A=1,3,5}^t$ v.s. β_0 for the XXZ chain of (22) by comparing with a p-GGE specified only by β_0 . The thermalization hypothesis also works well for $A = 1$ (red squares), but it worsens as A increases, i.e., $A = 3$ (blue circles) and $A = 5$ (black triangles). (b) Demographics of the typical states classified by the $\langle Q_0 \rangle$.

- [13] S. Goldstein, J. L. Lebowitz, R. Tumulka, and N. Zanghi, Canonical Typicality, *Phys. Rev. Lett.* **96**, 050403 (2006), [arXiv:cond-mat/0511091](#).
- [14] W. H. Zurek, Pointer Basis of Quantum Apparatus: Into What Mixture Does the Wave Packet Collapse?, *Phys. Rev. D* **24**, 1516 (1981).
- [15] S. Popescu, A. J. Short, and A. Winter, Entanglement and the foundations of statistical mechanics, *Nature Physics* **2**, 754

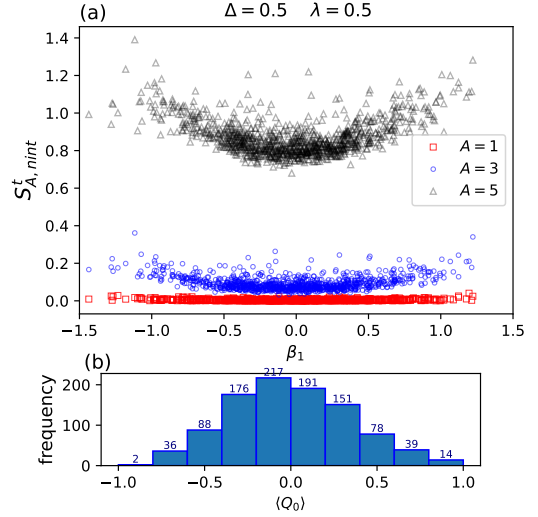


FIG. 22. (a) Typical-state thermalization demographics: $S_{A=1,3,5}^t$ v.s. β_1 for the XXZ spin chain of (22) by comparing with a p-GGE specified only by β_1 . The thermalization hypothesis also works well for $A = 1$ (red squares), but it worsens as A increases, i.e., $A = 3$ (blue circles) and $A = 5$ (black triangles). (b) Demographics of the typical states classified by the $\langle Q_0 \rangle$.

(2006).

- [16] M. P. Mueller, E. Adlam, L. Masanes, and N. Wiebe, Thermalization and canonical typicality in translation-invariant quantum lattice systems, *Commun. Math. Phys.* **340**, 499 (2015), [arXiv:1312.7420 \[quant-ph\]](#).
- [17] G. Biroli, C. Kollath, and A. M. Läuchli, Effect of rare fluctuations on the thermalization of isolated quantum systems, *Phys. Rev. Lett.* **105**, 250401 (2010).
- [18] T. Mori, Weak eigenstate thermalization with large deviation bound, [arXiv:1609.09776 \[cond-mat.stat-mech\]](#).
- [19] E. Iyoda, K. Kaneko, and T. Sagawa, Fluctuation theorem for many-body pure quantum states, *Phys. Rev. Lett.* **119**, 100601 (2017).
- [20] S. He, F.-L. Lin, and J.-j. Zhang, Dissimilarities of reduced density matrices and eigenstate thermalization hypothesis, *Journal of High Energy Physics* **12**, 073 (2017), [arXiv:1708.05090 \[hep-th\]](#).
- [21] P. Basu, D. Das, S. Datta, and S. Pal, Thermality of eigenstates in conformal field theories, *Phys. Rev. E* **96**, 022149 (2017), [arXiv:1705.03001 \[hep-th\]](#).
- [22] W.-Z. Guo, F.-L. Lin, and J. Zhang, Note on ETH of descendant states in 2D CFT, *Journal of High Energy Physics* **01**, 152 (2019), [arXiv:1810.01258 \[hep-th\]](#).
- [23] A. Dymarsky and K. Pavlenko, Generalized Eigenstate Thermalization Hypothesis in 2D Conformal Field Theories, *Phys. Rev. Lett.* **123**, 111602 (2019), [arXiv:1903.03559 \[hep-th\]](#).
- [24] L. Chen, A. Dymarsky, J. Tian, and H. Wang, Subsystem entropy in 2d CFT and KdV ETH, (2024), [arXiv:2409.19046 \[hep-th\]](#).
- [25] N. Yunger Halpern, P. Faist, J. Oppenheim, and A. Winter, Microcanonical and resource-theoretic derivations of the thermal state of a quantum system with noncommuting charges, *Nature Commun.* **7**, 12051 (2016).
- [26] C. Murthy, A. Babakhani, F. Iniguez, M. Srednicki, and N. Y. Halpern, Non-Abelian Eigenstate Thermalization Hypothesis,

- [Phys. Rev. Lett. **130**, 140402 \(2023\)](#), [arXiv:2206.05310 \[quant-ph\]](#).
- [27] N. Yunger Halpern, M. E. Beverland, and A. Kalev, Noncommuting conserved charges in quantum many-body thermalization, [Phys. Rev. E **101**, 042117 \(2020\)](#).
- [28] S. Majidy, W. F. Braasch, A. Lasek, T. Upadhyaya, A. Kalev, and N. Y. Halpern, Noncommuting conserved charges in quantum thermodynamics and beyond, [Nature Rev. Phys. **5**, 689 \(2023\)](#), [arXiv:2306.00054 \[quant-ph\]](#).
- [29] A. Lasek, J. D. Noh, J. LeSchack, and N. Y. Halpern, Numerical evidence for the non-Abelian eigenstate thermalization hypothesis, (2024), [arXiv:2412.07838 \[quant-ph\]](#).
- [30] T. Upadhyaya, W. F. Braasch, Jr., G. T. Landi, and N. Y. Halpern, Non-Abelian Transport Distinguishes Three Usually Equivalent Notions of Entropy Production, [PRX Quantum **5**, 030355 \(2024\)](#), [arXiv:2305.15480 \[quant-ph\]](#).
- [31] E. Cáceres, S. Eccles, J. Pollack, and S. Racz, Generic ETH: Eigenstate Thermalization beyond the Microcanonical, [arXiv:2403.05197 \[quant-ph\]](#).
- [32] Y. Guryanova, S. Popescu, A. J. Short, R. Silva, and P. Skrzypczyk, Thermodynamics of quantum systems with multiple conserved quantities, [Nature communications **7**, 12049 \(2016\)](#).
- [33] N. H. Y. Ng and M. P. Woods, Resource theory of quantum thermodynamics: Thermal operations and second laws, in *Thermodynamics in the quantum regime: Fundamental aspects and new directions* (Springer, 2019) pp. 625–650.
- [34] F.-L. Lin and C.-Y. Huang, Work statistics for quantum spin chains: Characterizing quantum phase transitions, benchmarking time evolution, and examining passivity of quantum states, [Phys. Rev. Res. **6**, 023169 \(2024\)](#), [arXiv:2308.13366 \[cond-mat.stat-mech\]](#).
- [35] A. Yuste, C. Cartwright, G. D. Chiara, and A. Sanpera, Entanglement scaling at first order quantum phase transitions, [New Journal of Physics **20**, 043006 \(2018\)](#).
- [36] L. F. Santos and E. J. Torres-Herrera, Nonequilibrium quantum dynamics of many-body systems, Chaotic, Fractional, and Complex Dynamics: New Insights and Perspectives , 231 (2018), [arXiv:1706.02031](#).